Free Surface Hydrodynamics of Submarine Masts Configurations

Giuliano VERNENGO [a,1], Stefano GAGGERO [a], Diego VILLA [a],
Giorgio MAZZARELLO [b], and Paola GUALENI [a]

[a] *Department of Electrical, Electronic and Telecommunications Engineering and Naval Architecture (DITEN), University of Genoa, Via Montallegro 1, 16145, GE, Italy*
[b] *Navy Ships Division, Fincantieri s.p.a., Via Cipro 11, 16129, GE, Italy*

Abstract. Sailing at snorkel depth is a necessary but dangerous operating scenario for submarines. The main and straightforward reason is that such an operating condition represents a time of possible vulnerability of the vessel. From a design perspective this condition affects the so-called *indiscretion rate*, that is exactly the ratio between this time of greater vulnerability and the total operating time. Moreover, when the vessel operates at snorkel depths there are some relevant operations that might be accomplished related to both snorkeling, communications and threats detection. These operations are typically carried out by using a certain number of masts, of slightly different shapes and sizes, that might be used in various configurations. The proposed study aims at providing some insights into the unsteady, turbulent, hydrodynamics of several submarine masts configurations. The analysis is carried out in terms of behaviors of the developed free surface, considering the nonlinear interactions rising among the masts considered. The maximum height and length of the breaking wave generated at the bow of each mast is analyzed. Both the near field and the far field unsteady wave patterns are discussed comparing several configurations and focusing on the interaction effects. The computational study is carried out by using an open-source Smoothed Particle Hydrodynamic solver called DualSPHysics, able to exploit the computational acceleration provided by GP-GPU cards.

Keywords. Surface-piercing cylinders, Submarine, Computational Fluid Dynamics (CFD), Smoothed Particles Hydrodynamics (SPH), Turbulent wake

1. Introduction: Submarine Hydrodynamics at Snorkel Depth

When a submarine sails at snorkel depth it is usually performs some operations involving one or more of its masts and antennas. Typical equipment is made of radar, search and attack periscopes, optronic antennas, other common masts and the snorkel. The latter is usually the thicker while the periscopes can be the thinner ones. These masts might be raised alone, or in a kind of tandem configuration, so aligned along a longitudinal axis, or staggered, having a lateral displacement with respect to each other. Hence, depending on the selected configuration the hydrodynamic interactions among the masts might generate very complex free surface flows. In addition to this relatively complex flow generated

---

[1] Corresponding Author: giuliano.vernengo@unige.it.

by the presence of multiple surface piercing, cylinders there is also the presence of the steady wave pattern created by the underwater hull moving close to the free surface.

In the present study this latter phenomenon has been ignored and a basic analysis of the wake of different masts configurations has been carried out. There are some relevant phenomena involved into submarine masts design that might be addressed to achieve the best possible performance, reducing as much as possible the visibility of the vessel in such a particular, and vulnerable, operating condition. Among these phenomena there is the wake formation and development behind the submarine or the undesired possibility of water overflow inside the snorkel mast. In any case, a very unsteady wave pattern is generated, usually characterized by a continuous breaking wave in front of the masts and by a highly turbulent wake behind them.

There are some quite recently published experimental results dealing with surface-piercing cylinders (1; 2; 3; 4). There are much more studies dealing with numerical simulations, by using e.g. RANS (5), LES (6) and DES (7), but none considering Smoothed Particles Hydrodynamics (SHP) as a method to solve such a type of problem, even if it is particularly suitable to deal with highly non-linear wave transformations (8) and wave-structure interactions (9).

2. Smoothed Particle Hydrodynamics Approach in DualSPHysics

The open-source SPH solver DualSPHysics (10), relying on the original formulation by (11) has been developed to exploit GP-GPU acceleration, including many features such as non-linear wave generation (12), dynamic boundary conditions (13) and coupling algorithms to solve specific problems (14; 15). A mesh-free Lagrangian framework is used to resolve the flow hydrodynamics based on particles description. The field variables such as V, ρ and p, as well as their derivatives, are represented in a continuous integral form by a suitable *kernel approximation* and then discretized over the computational domain through a so-called *particle approximation*. The values on a specific particle are then computed based on the nearest neighbor particles, according to the kernel formulation. An integral representation can be associated to a function $f(x)$ according to Eqs. (1). Using a kernel $W(x-x',h)$ relying on a smoothing length h, Eqs. (2) is the Kernel approximation of Eqs. (1). The cubic spline kernel function has been used in the proposed study.

$$f(x) = \int_\Omega f(x')\delta(x-x')dx' \tag{1}$$

$$\langle f(x)\rangle = \int_\Omega f(x')W(x-x',h)dx' \tag{2}$$

Pressure field is computed assuming that water is a weakly compressible fluid, then using the state equation, Eqs. (3), being c_0 is the sound speed ranging from 50 m/s up to 250 m/s to ensure $Mach < 0.1$ and γ is a constant equal to 7 for most of the problems. The mass and the momentum conservation laws, Eqs. (4) and Eqs. (5), respectively, can be written in terms of particles approximation.

$$p = \frac{c_0^2 \rho_0}{\gamma} \left[\left(\frac{\rho}{\rho_0} \right)^\gamma - 1 \right] \tag{3}$$

$$\frac{d\rho_i}{dt} = \sum_{ij} m_j (u_i - u_j) \nabla_i W_{ij} \tag{4}$$

$$\frac{d\mathbf{u}_i}{dt} = -\sum_{ij} m_j \left(\frac{P_i}{\rho_i^2} - \frac{P_j}{\rho_j^2} + \Pi_{ij} \right) \nabla_i W_{ij} + g \tag{5}$$

The summation over the two indexes i and j indicates the particles interactions; m, u and P are the particle mass, velocity and the pressure at a particle respectively. Π_{ij} is a force contribution used to avoid tensile instabilities. No turbulence models have been used but a so-called artificial viscosity approach, depending on a coefficient α, that is the main parameter that controls the additional force term Π_{ij}. A further diffusive term is introduced in the continuity equation as proposed by the *delta-SPH* formulation (16) in order to reduce density fluctuations generated by the combination of the stiff density field described by the state equation and the natural chaotic behaviour of the particles, resulting in high-frequency low amplitude oscillations in the density field.

The method has already been validated on a similar problem, i.e. the unsteady flow over a vertical surface-piercing NACA 0024 strut (9), providing reliable predictions of the average free surface elevation both close and far from the strut. It has also been successfully applied by the authors to other ship hydrodynamics related problems such as sloshing in anti-roll tanks (17) and slamming of wedge sections (18).

3. Analysis of Different Masts Configurations

The proposed preliminary analysis of a submarine masts hydrodynamics focuses on the shape of the turbulent wake behind the masts, with particular attention to changes of such a wake based on the selected configuration, and on assessing the capability of the SPH approach to handle the prediction of possible overflow at the top of the snorkel. To this aim, considering a possible masts and antennas configuration of a conventional submarine, as shown in Figure 1, the periscope alone, the snorkel alone and a three masts staggered configuration have been studied. The difference between the first and the second analysis is that the periscope has a thinner elliptic section compared to the cylindrical one of the snorkel. Moreover, four snorkel designs have been analyzed with respect to the overflow problem. Considering the purely cylindrical snorkel as the reference shape, an end plate has been added in the design S#2, another lower plate has been included in the design S#3, while a bow-like shape has been created for the design S#4. This preliminary study is aimed at proofing the capability of the proposed approach for the hydrodynamic design of such devices.
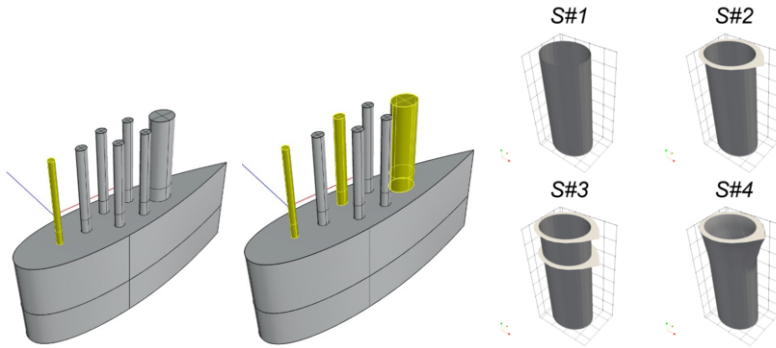
Figure 1. Mast's configurations. Left to right: periscope alone; periscope, antenna and snorkel (staggered); different snorkel designs.

3.1. Periscope

The attack periscope is usually located at the front of the masts system and it can be anyway used alone. It is typically characterized by a tiny elliptic or cylindrical section. The latter has been selected for the present study, considering a diameter equal to $D = 0.20m$. Figure 2 displays the free surface elevation, at $t \cdot U/D = 100$, obtained for the periscope advancing at three different, increasing, speeds, corresponding to $Fn_D = [1.43; 2.14; 2.86]$. The particle velocities at the free surface are shown by the colormap, increasing from blue to red. The wake behind the surface-piercing cylinder changes a lot with the speed. In particular, at the lower speed there is a relatively large turbulent, unstable, wake mostly concentrated behind the cylinder itself, with a maximum thickness of about $2 \cdot D$. As the speed increasing, at the intermediate speed, it starts the formation of a breaking bow wave while the turbulent wake behind the cylinder is contracted for about a length of $L_{wake} = 1.5 \cdot D$ before spreading into a divergent wave breaker that, despite unstable, follows the cylinder like a stationary wave. At the maximum speed the wave breaking at the bow of the cylinder is much more visible and wider, if compared to the previous case. The wake field behind the periscope present a longer contracted wake, in the extent of about $3.5 \cdot D$. The divergent wave front resulting from the spreading of the far-field turbulent wake shows a higher angle of propagation of the wave, with respect to the center plane of the domain, then covering a narrower portion of the free surface.

3.2. Snorkel Designs

The snorkel, contrary to the periscope, has a thicker section, typically elliptic, and is usually located to be the last mast of the sail. The main problem related to its hydrodynamic performance, beyond the wake formation that should be in principle as reduced as possible for all of the submarine masts, is the reduction of the overflow from its top head. Indeed, the snorkel top head is usually taken as closer as possible to the free surface, with the clear risk of water entry from the top e.g. due to combination of submarine motions and free surface waves. The four created designs are exactly meant to reduce or, at least, modify the height of the bow wave in front of the snorkel, then reducing the occurrence of the overflow. Considering the wake field behind the four snorkel designs, shown in
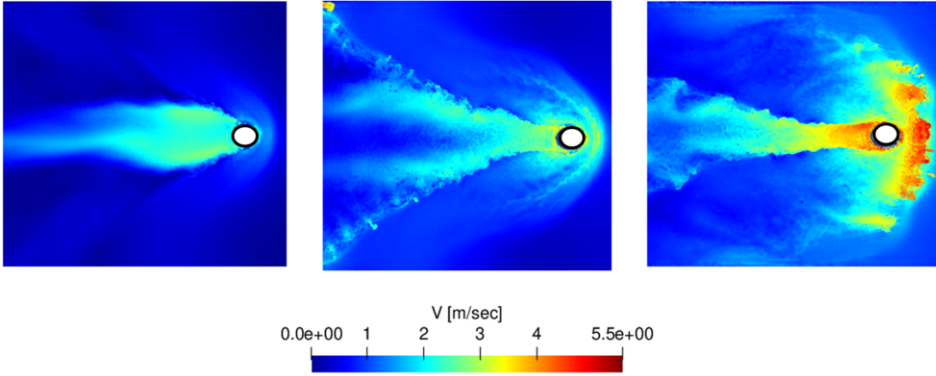
Figure 2. Turbulent wake for the periscope. Left to right: $Fn_D = [1.43; 2.14; 2.86]$. $t \cdot U/D = 100$.
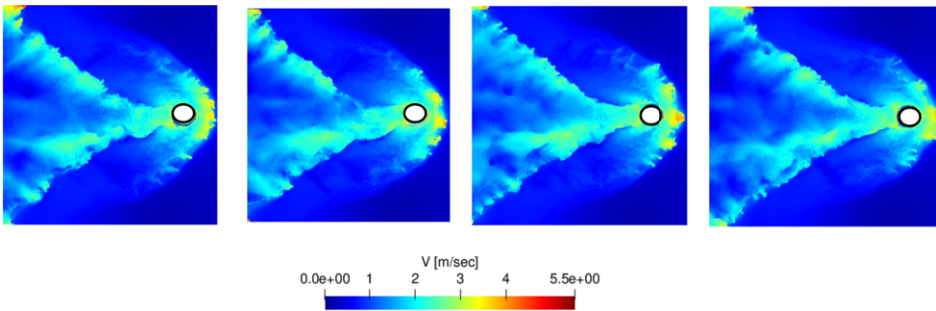

Figure 3. Turbulent wake for the four snorkel designs. Left to right, S#1 to S#4. $t \cdot U/D = 100$.

Figure 3 at the intermediate speed, no significant differences are found. Figure 4 displays the envelopes of the maximum wave heights at the longitudinal symmetry plane in front of the snorkel. Such envelopes have been computed by considering the bow wave profiles at all the time steps of a SPH simulation, translated into the origin of a reference system located exactly at the foremost point of the snorkel. The design S#2 is not reported because it is equal to the S#1, since at that speed the bow wave is always lower than the top of the snorkel. The purely cylindrical design presents the higher value of the bow wave envelope, equal to $\eta/c = 3.33$. The presence of the lower plate of the design S#3 reduces the height of the bow wave envelope to $\eta/c = 3.25$, that is about 2.5% lower. The larger reduction if found by using the snorkel design S#4, with a bow-like shape, resulting in $\eta/c = 3.18$ at the mast bow profile, i.e. reaching a reduction of -4.5% with respect to the reference design.

3.3. Staggered, 3 Masts, Configuration

The last configuration analyzed is made of three staggered masts. This can be made of e.g. the periscope and the snorkel, aligned at the longitudinal symmetry plane, plus an antenna located in between the two but with a given transverse shift with respect to the center plane. The antenna has similar dimensions as the periscope ones. In this

configuration, there are very strong free surface interactions among the three masts. In particular, the wake of the foremost cylinders do not have enough space to fully develops but they affect the wake of the following mast, as shown in Figure 5. The result is globally a contraction of the wake, that is more visible if this staggered configuration is compared to the periscope and the snorkel, as in Figure 6. The turbulent wake behind the staggered configuration is clearly narrower than both that of the periscope and the snorkel, partially due to the higher velocities obtained at the free surface for the presence of the different cylinders. The divergent wave front seem to disappear while there is the inception of a Karman vortex street due to the asymmetric interactions of the wakes of the three masts.
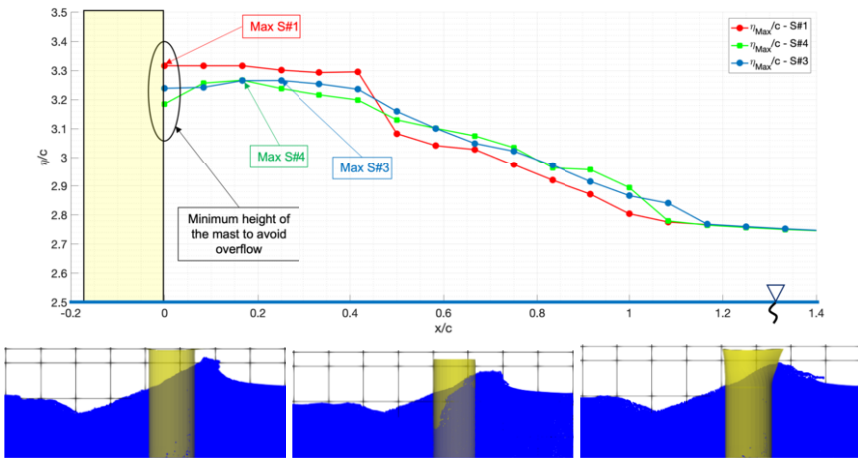

Figure 4. Comparison of the maximum bow wave elevation at the snorkel. Top: envelope of the max waves. Bottom, left to right: instantaneous wave elevation at the longitudinal symmetry plane, for the snorkel S#1, S#3 and S#4, at $t \cdot U/D = 100$.
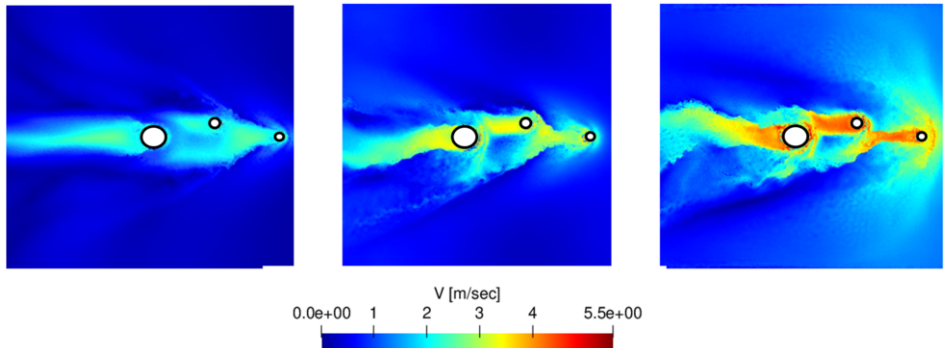

Figure 5. Turbulent wake for staggered masts configuration. Left to right: $Fn_D = [1.43; 2.14; 2.86]$. $t \cdot U/D = 100$.
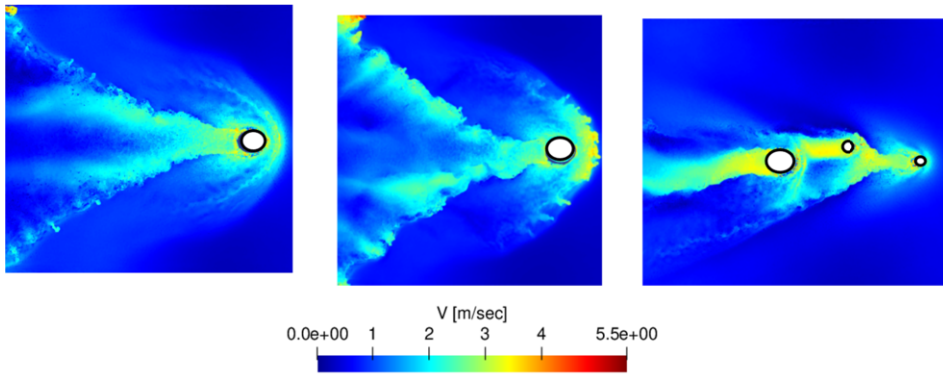
Figure 6. Turbulent wake for the four snorkel designs. Left to right: Periscope, Snorkel S#1, staggered masts. $t \cdot U/D = 100$.

4. Conclusions

A Smoothed Particles Hydrodynamics method has been used to study the hydrodynamic performance of a possible mast system for a conventional submarine design. The capability of this CFD approach to handle complex hydrodynamic free surface interactions and to predict changes in turbulent wake formation due to speed, shape and configuration variations, has been proven. The preliminary analysis focused on the turbulent wake development and on the bow wave height for different mast configurations and shapes. The shape of the turbulent wake has been properly characterized and the height of the wave breaker at the snorkel bow profile has been predicted for four deigns. It has been found that the possibility of overflow occurrence can be reduced by properly design the shape of the snorkel mast. Moreover, in terms of far field wake, the staggered configurations seems to produce the better effects, by introducing a relatively high transverse contraction and the presence of a Karman vortex street.

5. Acknowledgments

References

[1] Chaplin JR, Teigen P. Steady flow past a vertical surface-piercing circular cylinder. Journal of Fluids and Structures. 2003;18(3-4):271-85.

[2] Benitz MA, Carlson D, Seyed-Aghazadeh B, Modarres-Sadeghi Y, Lackner M, Schmidt D. CFD simulations and experimental measurements of flow past free-surface piercing, finite length cylinders with varying aspect ratios. Computers & Fluids. 2016;136:247-59.

[3] Potts DA, Binns JR, Marcollo H, Potts AE. Hydrodynamics of towed vertical surface-piercing cylinders. In: International Conference on Offshore Mechanics and Arctic Engineering. vol. 58769. American Society of Mechanical Engineers; 2019. p. V001T01A024.

[4] Ageorges V, Peixinho J, Perret G, Lartigue G, Moureau V. Experiments and Simulations of Free-Surface Flow behind a Finite Height Rigid Vertical Cylinder. Fluids. 2021;6(10):367.

[5] El Moctar O, Bertram V. RANSE simulations for high-Fn, high-Rn free-surface flows. In: 4th Numerical Towing Tank Symposium (NuTTS), Hamburg; 2001. .

[6] Yu G, Avital E, Williams J. Large eddy simulation of flow past free surface piercing circular cylinders. Journal of Fluids Engineering. 2008;130(10).

[7] Zhang J, Liang D, Fan X, Liu H. Detached eddy simulation of flow through a circular patch of free-surface-piercing cylinders. Advances in Water Resources. 2019;123:96-108.

[8] Roselli RAR, Vernengo G, Brizzolara S, Guercio R. SPH simulation of periodic wave breaking in the surf zone-A detailed fluid dynamic validation. Ocean Engineering. 2019;176:20-30.

[9] Vernengo G, Roselli RAR, Brizzolara S, Guercio R. Unsteady hydrodynamics of a vertical surface piercing strut by sph simulations. In: The 29th International Ocean and Polar Engineering Conference. OnePetro; 2019. .

[10] Domínguez JM, Fourtakas G, Altomare C, Canelas RB, Tafuni A, García-Feal O, et al. DualSPHysics: from fluid dynamics to multiphysics problems. Computational Particle Mechanics. 2021:1-29.

[11] Monaghan JJ. Smoothed particle hydrodynamics. Annual review of astronomy and astrophysics. 1992;30(1):543-74.

[12] Verbrugghe T, Domínguez JM, Altomare C, Tafuni A, Vacondio R, Troch P, et al. Non-linear wave generation and absorption using open boundaries within DualSPHysics. Computer Physics Communications. 2019;240:46-59.

[13] Tafuni A, Domínguez J, Vacondio R, Crespo A. A versatile algorithm for the treatment of open boundary conditions in Smoothed particle hydrodynamics GPU models. Computer Methods in Applied Mechanics and Engineering. 2018;342:604-24.

[14] Capasso S, Tagliafierro B, Martínez-Estévez I, Domínguez JM, Crespo AJ, Viccione G. A DEM approach for simulating flexible beam elements with the Project Chrono core module in DualSPHysics. Comp Particle Mechanics. 2022:1-17.

[15] Domínguez JM, Crespo AJ, Hall M, Altomare C, Wu M, Stratigaki V, et al. SPH simulation of floating structures with moorings. Coastal Engineering. 2019;153:103560.

[16] Molteni D, Colagrossi A. A simple procedure to improve the pressure evaluation in hydrodynamic context using the SPH. Computer Physics Communications. 2009;180(6):861-72.

[17] Papetti A, Vernengo G, Gaggero S, Villa D, Bonfiglio L. Smoothed particles hydrodynamics simulation of a U-tank in forced motion. In: PARTICLES VI: proceedings of the VI International Conference on Particle-Based Methods: fundamentals and applications. CIMNE; 2019. p. 806-15.

[18] Bonfiglio L, Gaggero S, Papetti A, Vernengo G, Villa D. Systematic analysis of mesh and meshless cfd methods for water impact problems. In: MARINE VII: proceedings of the VII International Conference on Computational Methods in Marine Engineering. CIMNE; 2017. p. 568-82.